World Applied Sciences Journal 30 (3): 366-375, 2014
ISSN 1818-4952

DOI: 10.5829/idosi.wasj.2014.30.03.14020

Polymer Melting in a Constant Depth Screw Channel

Nataliia Mihailovna Trufanova and Aleksei Grigorievich Shcherbinin

Perm National Research Polytechnic University, 29 Komsomolsky ave., 614990, Perm, Russia

Abstract: A theory of heat and mass transfer is developed to describe polymer melting in plasticating extruders. The proposed approach is based on the solution of the system of equations of conservation of mass, momentum and energy. The numerical solution to the system of differential equations is found by applying the alternating direction method. The system of algebraic equations is solved by the sweep method. For plasticating extruders with a constant depth channel, some interesting results have been obtained that provide a deeper understanding of the process of melting. An analysis is performed that accounts for the rate of melting at the melt film-solid bed interface, the shape of a polymer bed and the temperature and velocity distributions. Technological parameters, rheological, physical and geometrical factors are examined to study their influence on the rate of polymer melting and the length of the melting zone. It is concluded that energy dissipation markedly affects the melting process.

Key words: Plasticating extruder · Screw · Polymer · Mathematical model · The melting zone

INTRODUCTION

In Part I of this investigation [1], we described the state of the art of the problem of polymer melting in extruders and presented the model capable of describing the melting of a polymer granulate in the extruder channel. The model has its origin in the fundamental equations of conservation.

In the present work, we will discuss the numerical results for the melting zone of a constant depth channel using the notation accepted in Part I. The polymer examined in this study was fine-grained polycaproamide of various molecular mass and mean melting temperature T_m=220°C. The polymer melt exhibited no viscosity anomaly up to the shear rate $\dot{\gamma} = 1000$ s^{-1}, i.e. it is a Newtonian fluid. The dependence of its viscosity [mu] on the dimensionless temperature $T = \overline{T}, T_m$ is approximated by the Reynolds law fairly well. Thus,

$$\mu = \mu_0 \exp(-\beta T),$$

where μ_0=*675* Pa·s, β=0.027°C^{-1} are the rheological constants and $\overline{T}$ is the true temperature of the polymer melt.

Table 1 gives the temperature dependence of density ρ, thermal conductivity *k* and specific heat *C* of polycaproamide.

In order to study the basic mechanisms of heat/mass transfer processes in the melting zone of the extruder, we used the extruder with a 63mm internal diameter barrel. The channel width $\overline{S}$ was 55mm, the helix angle [phi] was 17°50 and the channel depth $\overline{H}$ in the melting zone was constant and comprised 2.5mm. The radial clearances between the flights and the barrel were neglected.

DISCUSSION

The numerical data obtained for polycaproamide melting in the extruder channel of the above-mentioned geometry are summarized in Table 2. In the table, the number of the calculation variant represents a respective set of physical-rheological data, heat transfer conditions and operating regimes of the extruder. μ_0 is the viscosity coefficient of melted polycaproamide, V_0 is the circumferential velocity of the screw (the barrel velocity in reversed direction), *G* is the mass flow rate of the extruder, $T_{BI} = \overline{T}_{BI} / T_m$ is the dimensionless temperature of

Corresponding Author: Nataliia Mihailovna Trufanova, Grigorievich Shcherbinin Perm National Research Polytechnic University, 29 Komsomolsky ave., 614990, Perm, Russia.

Table 1: Density, thermal conductivity and specific heat of polycaproamide at various temperatures

T,°C	ρ, kg/m^3	k, watt/(m grad)	C,J/(kg grad)	T,°C	ρ, kg/m^3	k, watt/(m grad)	C, J/(kg grad)
20	1152	0.382	1914	160	1087	0.360	3149
30	1146	0.381	1973	170	1081	0.358	3313
40	1142	0.379	2030	180	1073	0.356	3497
50	1138	0.377	2090	190	1064	0.354	3677
60	1134	0.376	2153	200	1052	0.345	4124
70	1130	0.374	2221	210	1030	0.286	5049
80	1126	0.372	2297	220	993	0.243	3599
90	1122	0.371	2379	230	987	0.245	2365
100	1118	0.369	2464	240	982	0.246	2403
110	1113	0.368	2553	250	977	0.248	2428
120	1109	0.366	2651	260	974	0.250	2456
130	1104	0.364	2763	270	970	0.251	2489
140	1099	0.363	2873	280	667	0.253	2516
150	1093	0.361	3002				

Table 2: Operating conditions for extruded polycaproamide

variant no.	μ_0, Pa s	V_o, m/s	G, kg/s	T_{BI}	T_{Bm}	heat source	Re·10^{-3}	Pe	Ek·10^{-3}
1	675	0.251	0.020	1.24	1.24	T_B+D	0.957	6463	9.54
2	675	0.251	0.0056	1.24	1.24	T_B+D	0.957	6463	9.54
3	675	0.251	0.020	1.24	1.24	T_B	0.957	6463	9.54
4	675	0.251	0.020	1.24	1.24	T_B+D+T_0	0.957	6463	9.54
5	1845	0.296	0.022	1.34	1.34	T_B+D	0.330	6098	13.30
6	1100	0.296	0.022	1.34	1.34	T_B+D	0.554	6098	13.30
7	675	0.296	0.022	1.34	1.34	T_B+D	0.903	6098	13.30
8	1845	0.251	0.0056	1.24	1.24	T_B+D	0.957	6463	9.54
9	675	0.251	0.020	1.33	1.33	T_B+D	0.957	6463	9.54
10	675	0.176	0.020	1.24	1.24	T_B+D+T_0	0.671	4532	4.69
11	675	0.325	0.020	1.24	1.24	T_B+D+T_0	1.24	8369	16.00
12	675	0.251	0.020	1.24	1.24	T_B+D	0.957	12926	9.54
13	675	0.251	0.020	1.60	1.60	T_B+D	0.957	6463	9.54
14	675	0.251	0.0056	1.24	1.24	T_B	0.957	6463	9.54

the barrel in the feeding zone, $T_{Bm} = \overline{T}_{Bm} / T_m$ is the dimensionless temperature of the barrel in the melting zone, Pe, Re, Ek are the Pecle, Reynolds and Ekkert (see work [1]).

In the column "heat sources", T_B is the amount of heat derived from the heated barrel, D is the amount of dissipative heat and T_0 is the preheating temperature of a granulate prior its feeding into the extruder hopper.

The Shape and Sizes of a Solid Bed: Among the problems associated with polymer melting, a good understanding of the true mechanism of melting is of primary interest. Tadmor's melting theory [2] proceeds from the two basic assumptions: a) the interface is rectangular and b) melting occurs on one side of a solid bed only. The mechanism of polymer melting in the extruder channel (variant 1, Table 2) is illustrated in Figure 1. The origin of the longitudinal coordinate x is at the final part of the melting delay zone. Similar patterns were obtained for other melting conditions. The melting mechanism remains the same in all cases. The shape of a solid bed differs greatly from a rectangular form. Thus, it can be concluded that the material melting with different velocity occurs simultaneously over the entire curvilinear interface.

The above conclusion has been supported by the experimental results obtained for polymer melting under extrusion [3-7]. The melting mechanism can be represented as follows. Heat spent on polymer heating and melting is conducted into the melt from two sources-external and internal. The latter caused by viscous dissipation acts at every point of the melt. The energy supplied and produced is redistributed and conducted into the interface owing to the convective and molecular mechanisms of heat transfer. However, because of the poor thermal conductivity of polymer materials and the intensive circulation of the melt

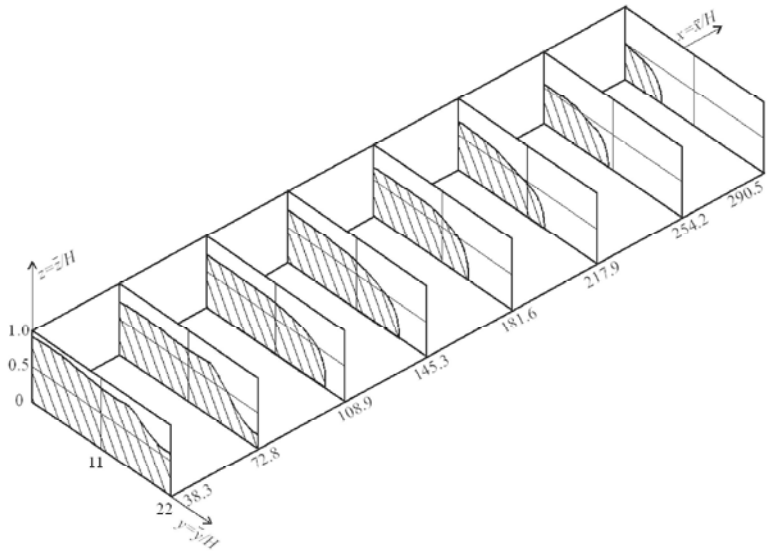

Fig. 1: Shape variations of a solid polymer bed along the extruder channel. (channel depth, H = 2.5 mm, channel width, S = 57 mm)

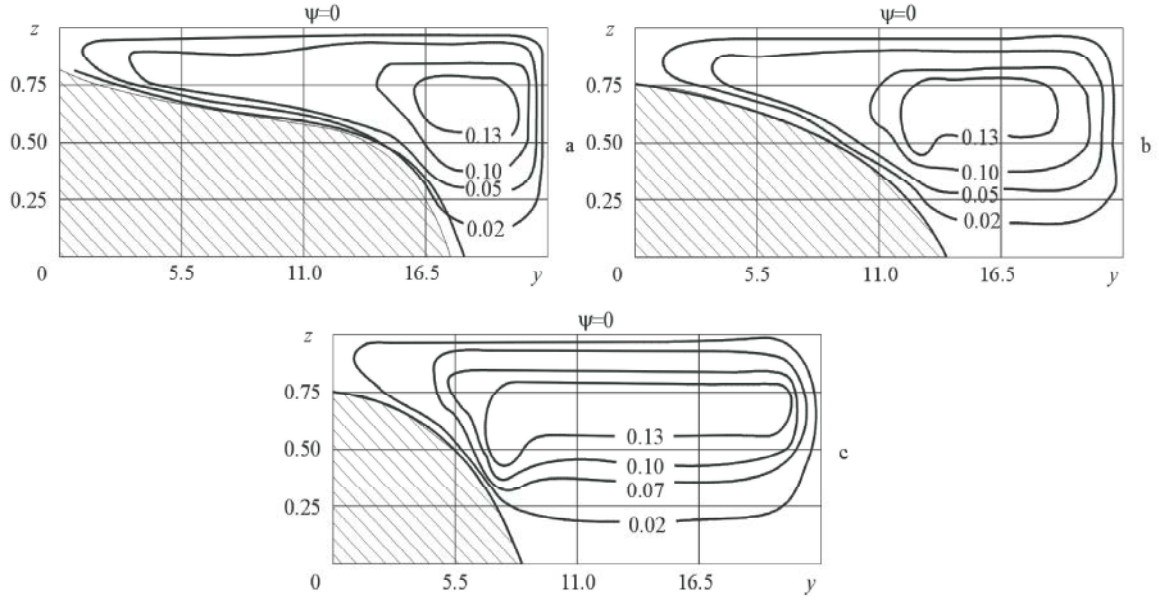

Fig. 2: Distribution of the flow function over the channel cross section: a-x = 146, b-220 and c-292.

(the best heated layers of the melt are carried away from the barrel surface and mixed with colder layers), the contribution of the molecular mechanism to the process of redistribution is insignificant. Thus, the convective heat transfer prevails over the diffusive one and, as a result, the hot melt flows constantly over all curvilinear interface and the melting takes place in all its points but at different velocity. The melt convection produces the zone of intensive melting at the channel bottom, where the hottest material is.

The circular flow generates a large vortex. The vortex shape and its movement along the channel are shown in Figure 2.

Tadmor, Klein and Maddock [8, 9] remarked that the solid bed shape, determined through visual observation, had a near rectangular cross-section. The discrepancy between the theoretical and experimental results was attributed to the experimental procedure. Upon reaching the operating conditions, the heating of the barrel was completed and the screw was

stopped. This was accomplished by rapid cooling the barrel (up to the full freezing of the melt). Then the barrel was slightly reheated (up to the formation of the melt film near the barrel surface) to push the screw out of the extruder. The freezing procedure took 10-15 minutes [8, 9]. Some conclusions on experiments were drawn based on the results of investigation of the frozen melt. To study the heat processes that took place during polymer solidification, the freezing was simulated numerically. The procedure was as follows. First, the problem of polymer melting was solved. Then, at the point in time, corresponding to a certain cross-section of the channel, all velocities became zero filled and the boundary condition for temperature on the moving surface changed. Only the heat conductivity equation was solved.

The numerical analysis of freezing showed that the intensive cooling of the barrel led to the formation of a near-surface solid layer that increased slowly because of its weak thermal conductivity. At the same time, owing to the heat accumulated in the melt, the solid bed continued to melt. The fastest melting was observed in the near-bottom area of the screw channel, where the most heat was accumulated. In the course of time, the stored heat was used up, the melting was completed and just the freezing of the melt proceeded. Since the period of time within which the initial melting took place was short (order of 2-4 seconds) with respect to the time of the experiment, the experimentalists examined the shape of a partially-melted polymer plug only. In this case, the solid bed shape was close to rectangular. In fact the experimental studies show [6] that the Tadmor's melting model describes the process of polymer melting in the plasticating extruder channel not in a proper way.

Numerical calculations of a variety of barrel temperatures (from 20 to 200°C) showed that the aforementioned patterns of polymer solidification remained practically unchanged. This could be explained by slow heat removal (low heatconductivity of the polymer) and short time of the melting mechanism. It should be noted that the theoretical studies were performed under more drastic conditions, i.e. the barrel temperature changed step-wise (from 270°C to 22°C). In real conditions, the temperature decreased gradually. In Figure 3, the solid line represents the bed shape prior cooling, the dashed lines-interfaces at various times. The shaded area confines the final shape of a solid bed. The results shown correspond to variant 1, Table 2 (T_0 = 22°C).

The Length of the Melting Zone: It is of interest to know how the frequency of screw rotation, the extruder throughput, the barrel temperature, the initial heating of a granulate, the dissipative source power and other parameters influence the melting of polymers and, in particular, the length of the melting zone. To evaluate the contribution of each of these factors to the melting process, numerical studies have been carried out under a variety of initial conditions (Table 2).

It is to be noted that earlier the obtained results were represented as a down channel variation of the relative width of a polymer bed. That is

$$y_0 = \frac{\bar{y}_0(x)}{S}, \quad (1)$$

where S is the channel width, $\bar{y}_0(x)$ is the largest width of a bed in the considered cross section.

Tadmor [10] was the first to introduce the parameter y_0 as a ratio of intensity of polymer melting. He followed from the assumption that the interface was rectangular. Chang in his work [4] pointed out that the value y_0 could not be used as such criterion. The results obtained with the aid of our model have confirmed the validity of Chang's conclusion. The melting at any point of the extruder channel can be best characterized by the rate of

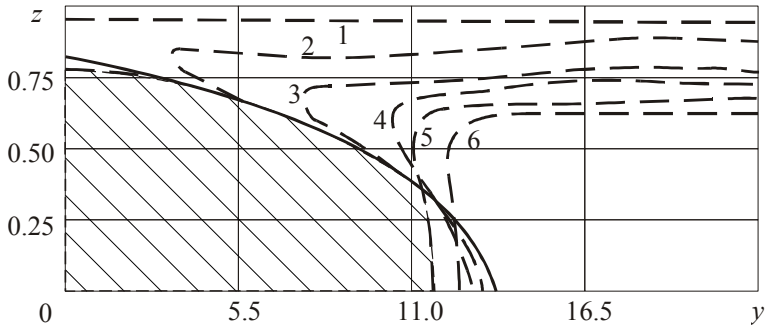

Fig. 3: Movement of the interface in the cooling experiment. 1-τ 2-21; 3-35; 4-49; 5-63; 6-70. Here $\tau=tv_0/H$

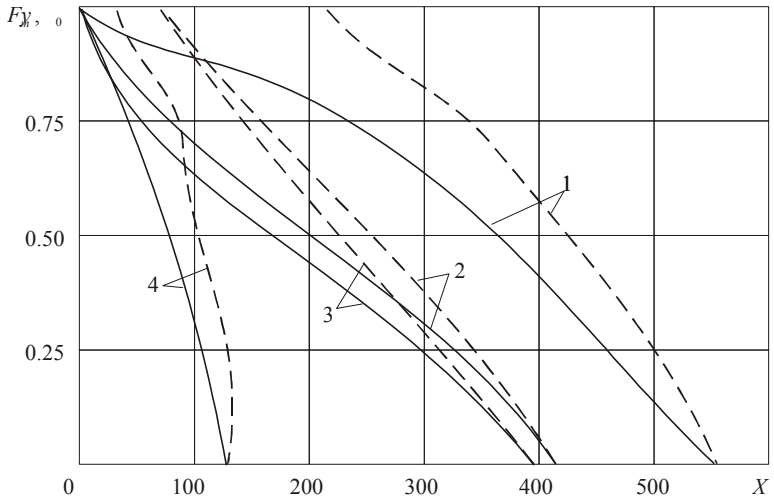

Fig. 4: Changes in the relative area F_m (solid lines) and the width y_0 (dashed lines) of a polymer bed along the melting zone. For additional information see the text

melting that will be considered later in detail. The melting can be readily illustrated by the dependence of the relative cross section of the solid bed on the longitudinal coordinate *x*.

$$F_m = \frac{F(x)}{F_0},$$

where *F(x)* and F_0 re the cross sections of the solid bed at the distance *x* from the entry into the melting zone and at the entry into this zone, respectively.

The effect of heat sources on the length of the melting zone is shown in Figure 4 (curves 1, 2, 3). As it was expected, the heating from internal and external heat sources and the preheating of the solid bed to 60°C led to the most intensive melting and, therefore, to the smallest length of the melting zone (curve 3). Comparison of curves 2 and 3 shows that the decrease in polymer heating to 40°C increases the length of the melting zone slightly. The heat that comes from the external heater (curve 1) leads to a 30-35% increase in the length of the melting zone. Energy dissipation makes significant contribution to the total heat balance and the melting process (curves 2 and 3). For a number of polymers and special-purpose extruders, the melting can only take place under the action of this heat source [11, 12]. The results presented in Figure 4 correspond to the following variants: curves 1-3, 2-1, 3-4, 4-2 (see Table 2).

The extruder throughput that defines the velocity of a solid bed influences essentially polymer melting, which can be represented as a combination of two interacted contradictory phenomena related to the capacity of internal and external heat sources and the time of heating. The lower the throughput and, as a result, the velocity of the bed, the higher the residence time of the polymer in the channel. Therefore, the polymer that is at the same distance from the entry and moves slowly is warmed up to much higher temperatures due to the longer action of external heating. On the other hand, the amount of heat coming from the internal (dissipative) heater decreases in a warmed and less viscous melt.

A several times decrease in the flow rate of the polymer leads to a longer stay of the polymer in the channel. The amount of heat delivered from the external source far exceeds that of undissipated heat. Therefore, for the bed moving at low velocity, the length of the melting zone is much smaller (curve 2 and curve 4 in Fig.4).

Figure 5 presents the shape of the solid bed for different cross-sections of the channel and under the action of the heat from various heat sources.

Curves 1 (variant 3) represent the bed shape formed under the action of the external heat, curves 2-heat delivered from the barrel and dissipation of the mechanical energy (variant 1). Curves 3 (variant 4)-heat delivered from the barrel, dissipation of the mechanical energy and granulate reheating. It is seen that the polymer melting goes faster in the last case.

One can assess the contribution of the internal heat source by changing the viscosity coefficient of the melt μ_0 Although there is a linear relation between them, the nonlinear temperature dependence of energy dissipation

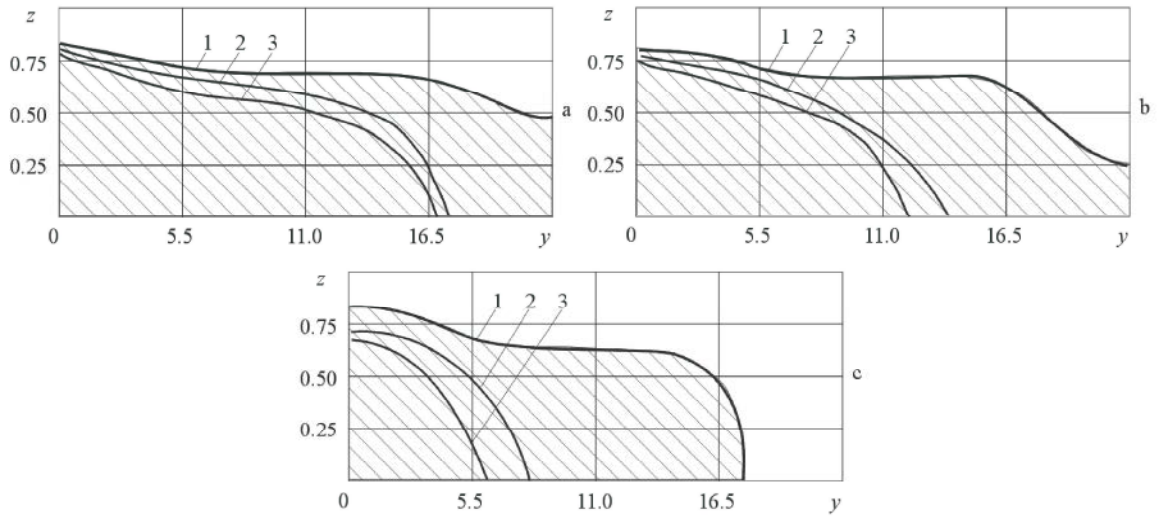

Fig. 5: Effect of source heaters on the shape and sizes of a polymer bed at different distances from the beginning of the melting zone: a-*x=146* ; b-220; c-292. For additional information see the text

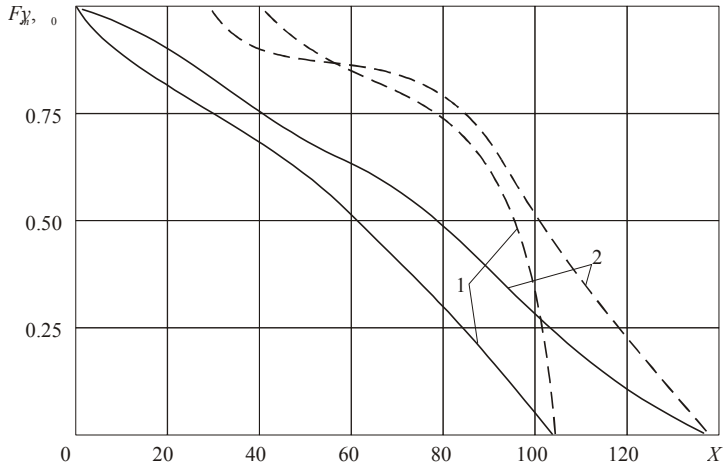

Fig. 6: Changes in the relative area *Fm* (solid lines) and relative width y_0 (dashed lines) of a polymer bed along the melting zone: 1-$\mu_0$1845Pa·s; 2-675.

suggests that if μ_0 increases by a factor of two or three, then the length of the melting zone decreases by14% or 22 %, respectively (variants 5, 6, 7). Similar results, i.e. the relationships between the viscosity and the resulting length of the melting zone, were also obtained for other initial data. Figure 6 (variants 2, 8) shows the change of the relative cross-section area of the bed F_m(solid curves) and its relative width y_0 dotted curves) along the melting zone depending on the value of the viscosity coefficient. Curves 1 correspond to μ_0 = 1845 Pa s and curves 2 to μ_0 = 675 Pa s. It is seen that with increasing $\mu_0$the length of the melting zone becomes smaller, though slightly.

The ambiguous and complex effect of the barrel temperature and the screw speed on melting can be attributed to the joint action of two heat sources, internal and external. The external heater power is independent of the temperature and properties of the polymer, the channel geometry and the extruder operation. The internal heater power depends first on these parameters and, what is more importantly, decreases with increasing the polymer temperature. This explains an increase in the length of the melting zone (Fig. 7, curve 1) and a decrease in the length of the feed zone (curve 2) with the barrel temperature. By the length of the feed zone we mean the part of the

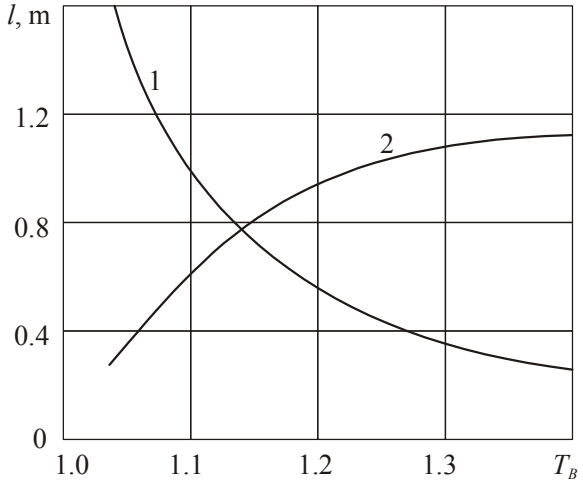

Fig. 7: Lengths of the feed (1) and melting zones (2) versus the dimensionless temperature of the barrel, $T_B = \overline{T}_B / T_m$

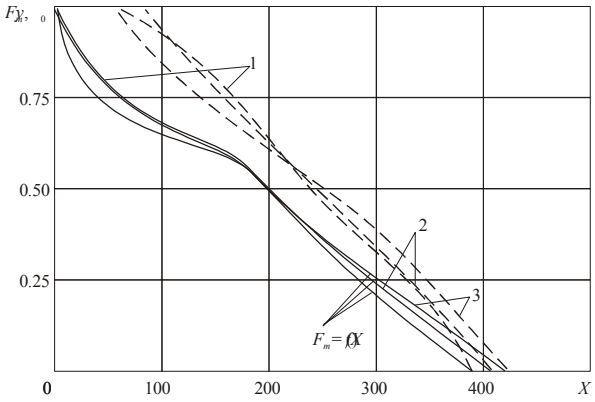

Fig. 8: Effect of the rotational speed of the screw on the length of the melting zone: 1 -v_0 = 0352 m/s, 2-0.251, 3-0.176

channel in which the heat transfer processes can be described by the conductivity equation. Curves from Figure 7 were plotted for variant 1.

As the rotational speed of the screw increases, the length of the melting zone decreases. However, the melting zone changes by only ±4% (Fig. 8, variants 4, 10, 11), when the rotational speed changes by ±30%.

Velocity Profiles of the Polymer Melt and down Channel Pressure Distribution: Figure 9 (variant 1) presents the characteristic distribution of the dimensionless velocities $v_y = \overline{v}_y / v_{0y}$, $v_z = \overline{v}_z / v_{0y}$, $v_x = \overline{v}_x / v_{0y}$ and temperature $T = \overline{T} / T_m$ at the distance $z = \overline{z} / H = 220$ $(\overline{z} = 0.55m)$ from the beginning of the melting zone. Here, v_y, v_z and v_x are the true melt velocities in the direction of the *y, z*

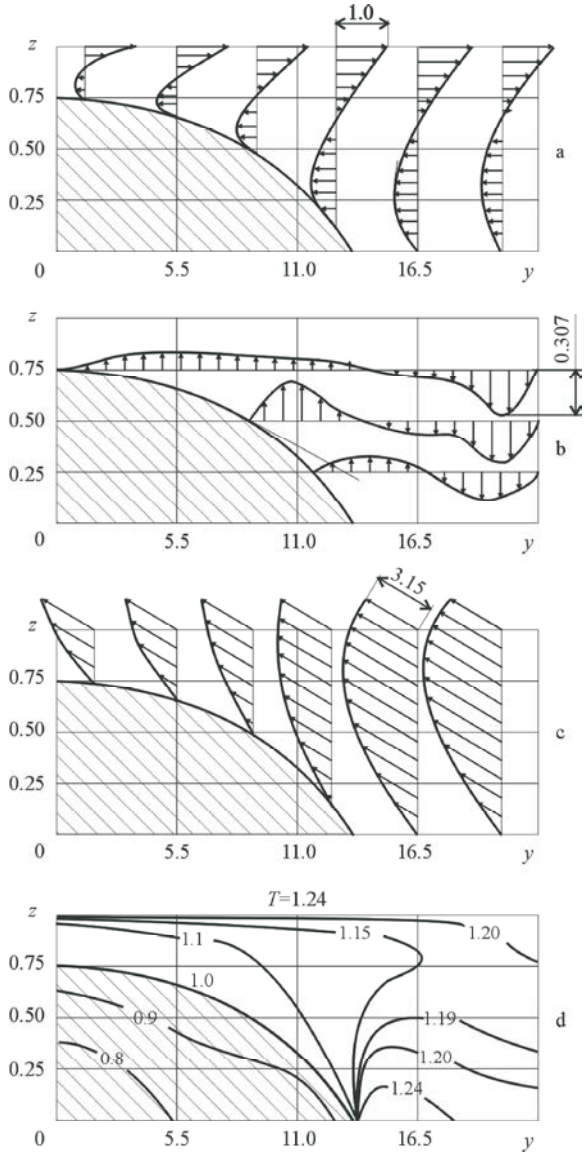

Fig. 9: Distribution of velocities v_y (a), v_z (b), v_x (c) and temperature *T*(*d*) over the channel cross section from the beginning of the melting zone at *x*=200

and *x*-axes and v_{0y} is the velocity component of the upper plate V_0 in the direction of the *y*-axis [8, 9]. The analysis of the velocity fields has verified the intensive circulation of the melt, at which the velocity v_z reaches, in wide channel portions, the values comparable with the value of v_x. Temperature distribution over the channel cross-section indicates that a solid bed consisting of granules was strongly warmed up in the course of its motion and melting along the channel axis. The regions with the highest temperature occur near the top hot surface of the barrel and at the channel bottom near the interface.

The proposed mathematical model of the polymer melting allows the calculation of down channel pressure distribution. Theoretically, one can easy determine the pressure in all four extruder zones, i.e. in the feed and melting delay zones and in the melting and metering zones. However, the first portion of the melt in the feed zone only partially fills the space between pellets and only slightly adheres to the internal barrel surface not generating the continuous flow. Therefore, the main problem is to define the channel cross-section with the continuously melted layer. By now, this important and complicated issue is poorly studied and, therefore, the calculation results obtained for pressure in the melting delay zone can not be recognized as entirely reliable. The point is that the pressure value is calculated with the accuracy to some constant, whose value depends on the location of the cross-section with the continuous melt flux. As is seen from the experiments [4], the melt, due to its high viscosity and the high packing density of the solid phase, is unable to penetrate deep inside the bed and the amount of the melt that fills voids is small.

Accordingly, the error of the distance from the entry to the aforementioned cross-section is small. Calculation results show that the order and pattern of the pressure change are in good agreement with the results provided in works [4, 13].

The numerical analysis of the pressure distribution and pressure gradient demonstrates that their values are dependent on the screw speed and extruder output. Indeed, since the mass flow rate of the polymer G and the velocity of a solid bed u are in one-to-one correspondence (the value of the last is constant), then the condition for constant flow rate can only be met at the expense of a change in the velocity of the melt. As the velocity of the upper boundary V_0 is much greater than that of a solid bed u, in the melting delay zone there occur high positive pressure gradients and the pressure increases dramatically.

When the polymer flows in the melting zone, two types of the melting flow are realized at different flow rates. In the case of the high flow rate and the channel height in the feed zone three or two times as much as the channel depth in the melting zone, the velocity of the melt increases sharply. Such growth of the melt velocity is possible at negative pressure gradients, which leads to the pressure decrease in the melting zone (curve 1, Fig. 10). At low flow rate, in the melting zone the sign of the pressure gradient remains unchanged and the pressure value along the melting zone increases (curve 2, Fig. 10). In Figure 10, the change in the pressure gradient and the down channel change of pressure are given in terms of the Euler numbers

$$\mathrm{Eu} = -\frac{H}{\rho v_{0y}^2}\frac{dp}{dx},\ \mathrm{Eu}_p = -\frac{\Delta p}{\rho v_{0y}^2}, \tag{3}$$

From (3) it follows that the values dp/dx and Eu have opposite signs. The minus sign of the number Eu_p (curve 1, Fig. 10) indicates a down channel pressure decrease.

Distribution of the dimensionless temperature, $T = \overline{T}/T_m$, over the cross-section of the screw channel is given in Figures 11 and 12 (variants 10 and 9). The curves are represented as isotherms. The temperature of the upper plate (the extruder barrel) is equal to the heating temperature and the interface temperature-to

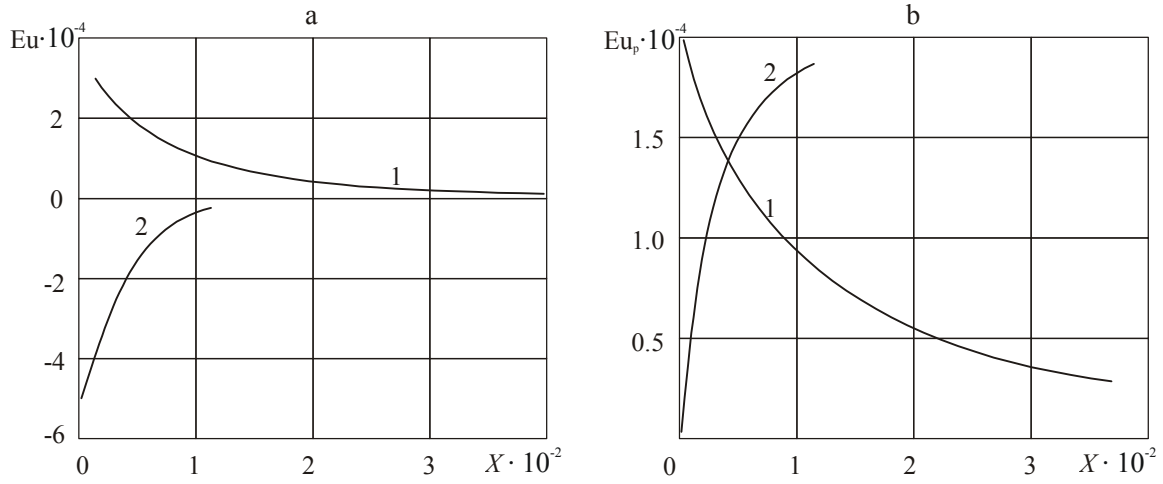

Fig. 10: Change in the pressure gradient (number Eu) and pressure (number Eu_p) along the melting zone: 1-G = 0.02 kg/s, 2-0.0056

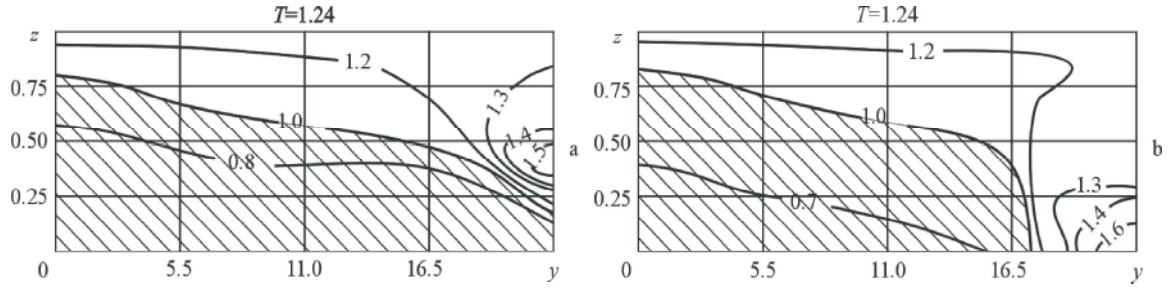

Fig. 11: Temperature distribution $T = \overline{T} / T_m$ over the channel cross-section: a-x =105, b-210. For additional information see the text.

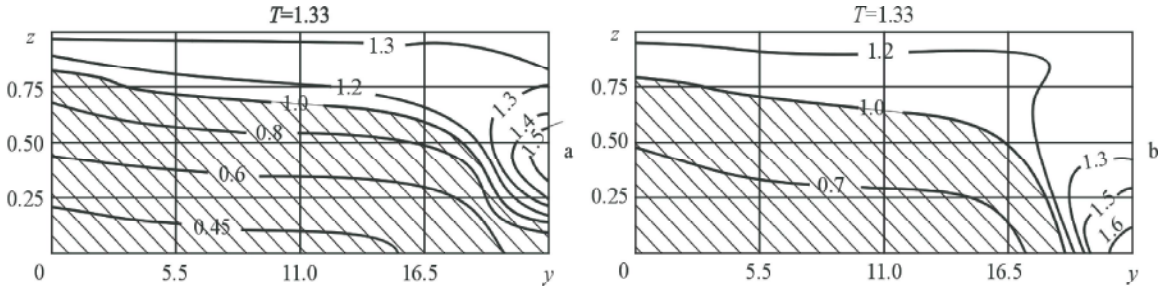

Fig. 12: Temperature distribution $T = \overline{T} / T_m$ over the channel cross-section: a-*x=146*; b-220. For additional information see the text

the temperature of polymer melting ($T = \overline{T} / T_m = 1$). It is seen that the "hot" regions of the melt are arranged near the left-hand side of the channel. As the polymer melts, these regions approach the channel bottom. Thus, we can say that the greatest overheat of the melt takes place in the extruder part where the solid bed has melt up to the channel bottom. The melt circulation generates the melt pool.

Temperature Distribution: A rise in the barrel temperature and in the rotation velocity of a screw (Figures 11 and 12) leads to the marked local overheat. Special attention must be given to high temperature gradients in the polymer melt (especially in the pool) and in the solid polymer bed. However, as the polymer bed moves to the discharge zone, its left-hand part continues to melt (this process is mainly caused by the elevated temperature of the melt in the pool). The melting region with the elevated temperature decreases and, in the long run, disappears completely. The lifetime of hot regions depends on the operating conditions of the extruder and the polymer properties. However, with properly calculated operating conditions, it is possible to get rid of local overheat. This procedure is of importance because overheating may cause polymer destruction and impair extrudate quality.

ACKNOWLEDGEMENT

This article was prepared under a grant of Russian Foundation for Basic Research #13-08-9603413.

Nomenclature:

x, y, z	=	coordinates
S	=	channel width
H	=	channel depth in feed and metering zones
V_0	=	barrel velocity
G	=	flow rate
c, k, [rho]	=	capacity, heat conductivity, density
[mu]	=	viscosity
μ_0, [beta]	=	rheological constants
T	=	temperature
v_x, v_y, v_z	=	velocity components
v_{0y}	=	velocity component of the upper plate V_0 in the direction of the *y*-axis
u	=	velocity of a solid bed
y_0	=	relative width of a polymer bed
F_m	=	relative cross section of the solid bed
V_m	=	melting temperature
T_{Bm}	=	dimensionless temperature of the barrel in the melting zone
E_{BI}	=	dimensionless temperature of the barrel in the feeding zone

I_2 = square invariant of the strain rate tensor
D = the amount of dissipative heat
T_0 = preheating temperature of a granulate

REFERENCES

1. Trufanova, N.M. and A.G. Shcherbinin, 2013. Problem Background and Mathematical Model of Polymer Movement and Melting. World Applied Sciences Journal, 27(11): 1401-1412.
2. Tadmor, Z. and K. Gogos, 1984. Theoretical backgrounds of polymer processing. Moscow.: Khimija, pp: 632.
3. Fukase, H., T. Nunoi, S. Shinia and A. Nemura, 1982. A plasticating model for single-screw extruder. Polymer Eng. Sci., 22(9): 578-586.
4. Mount, S.M. and C.J. Chang, 1978. Melting behavior of solid polymers on a metal surface at processing conditions. Polymer Eng. Sci., 18(9): 711-720.
5. Kellym, A.L., E.C. Brown and P.D. Coates, 2005. Melt temperature field measurement: influence of extruder screw and die geometry. Plastics, Rubber and Composites, 34(9): 410-416.
6. Cunha, S.M., A. Gaspar-Cunha and J.A. Covas, 2009. Melting of polymer blends in single-screw extrusion-an experimental study. Int. J. Mater Form, 2(1): 729-732.
7. Altinkaynak, A., M. Gupta, M.A. Spalding and S.L. Crabtree, 2011. Melting in a Single Screw Extruder: Experiments and 3D Finite Element Simulations. International Polymer Processing, 2: 182-196.
8. Tadmor, Z. and I. Klein, 1970. Principles of plasticating extrusion. New York: Van Nostrand Reinhold Co., pp: 479.
9. Moddock, B.H., 1959. SPE Jounal, 15(5): 383-389.
10. Tadmor, Z., 1966. PolymerEng.Sci., 3: 185-190.
11. MacKelvi, D.M., 1965. Polymer Processing, Moscow: Khimija, pp: 444.
12. Bernhardt, E.C., 1965. Processing of Thermoplastic Materials, pp: 747.
13. Donovan, R.G., 1971. Polymer Eng.Sci., 11(3): 247-257.